Mixing nanostructured Ni/piezoPVDF composite thin films with e-beam irradiation: A beneficial synergy to piezoelectric response

Natalia Potrzebowska [a], Olivier Cavani [a], Ozlem Oral [a], Olivier Doaré [b], Giuseppe Melilli [a,c], Jean-Eric Wegrowe [a,*], Marie-Claude. Clochard [a,*]

[a] *LSI, CEA-CNRS-Ecole Polytechnique, Institut Polytechnique de Paris, F-91120, PALAISEAU, France*
[b] *ENSTA, IMSIA, Institut Polytechnique de Paris, Boulevard des Maréchaux, F-91128, PALAISEAU, France*
[c] *Université Côte d'Azur, Institut de Chimie de Nice, UMR CNRS 7272, 06100, Nice, France*

A R T I C L E   I N F O

A B S T R A C T

Piezoelectric PVDF polymer thin films are nanostructured by swift heavy ion beam resulting in nanoporous structures. The nanocylindars are then partially filled with Ni(0) in order to create a composite of higher dielectric permittivity. In a second step, the composite is irradiated with electron beam, in order to induce chain scissions in the PVDF matrix and render it more flexible. It is found that e-beam irradiation does not affect the remanent polarization up to more than 1MGy. The energy harvesting properties are optimized with a maximum for 1MGy irradiation, delivering an output voltage of 4.1 V.cm^{-2} which corresponds to a maximum output power of 25μW. cm^{-2} and an integrated power of 0.46μW. cm^{-2} for 1 bar of external pressure (mechanical solicitations frequency of 10 Hz). The mechanisms responsible for the enhancement of the harvesting efficiency due to e-beam irradiation are discussed.

1. Introduction

In the trend of development of autonomous portable devices, energy harvesting including piezoelectricity appears to be the most promising approach to power wireless micro-devices. Among various materials used for energy harvesting [1,2], piezoelectric polymeric compounds compile several advantages such as flexibility and robustness. Moreover, they become really competitive in high deformation regime under severe environment (for e.g. wind generator or penstock pipe industry). The ideal polymer is polyvinyl difluoride (PVDF), a semi-crystalline polymer with well-known piezoelectric properties. PVDF is polymorph and presents five crystalline phases: α, β, γ, δ, and ε. The β phase is mainly responsible for the piezoelectric properties. [3–5] PVDF main inconvenience is its low relative permittivity, with the effect that small sensing elements will have low capacitances and suffer signal loss through electrical loading. To overcome this low-capacitance problem, nano-patterning and composite approaches have recently emerged and significantly improved both the dielectric permittivity of PVDF based materials and the energy harvesting by increasing the exchange surfaces [6,7]. Plethora of efficient piezoelectric nanogenerators for self-powered sensor based on modified β-PVDF including 1D nanostructuration

and/or inorganic nanoparticles fillers are still under study [6–13]. However, CVD and/or lithography techniques are usually involved in the fabrication steps. Moreover, rigid metallic oxide template may limit the deformation under severe strain, and an additional poling step is most of the time necessary to realign dipolar momentum in β-PVDF-based piezoelectric composites. All these processes impose industrial limitations for large-scale and low-cost production.

Quite recently, our research group [14] has shown that swift heavy ions (SHI) bombardment allows to nanostructure and fabricate by bottom-up processes embedded 1D inorganic nanowires (NWs) in commercially poled PVDF thin films. No PVDF depolarization occurs under irradiation [14,15]. This results in highly flexible and robust β-PVDF/Ni NWs composite thin films exhibiting 3D alignment of 1D Ni NWs with a density of 5.10^8 per cm^2 which increased by a factor 5 the dielectric permittivity. The piezopotential of resulted β-PVDF/Ni NWs composites was enhanced by a factor 2.5.

To go beyond, another important parameter driving the electromechanical constant of piezoelectric polymer materials is the elastic stiffness. Even if the complexity of the relationship between piezoelectric and elastic responses [16] is still under investigation, increased compliance stays one of the key factors and PVDF has already been

---

subjected to various modification approaches such as copolymerization with the most commonly used PVDF-*co*-TrFE or additives incorporation. A supplementary treatment was also proposed in 1998 by Zhang et al. [17] exposing PVDF based copolymer films to electron-beam (e-beam) irradiation for actuator and transducer applications. It was reported that e-beam induced defaults generated a giant electrostriction and relaxor ferroelectric behavior in PVDF-*co*-TrFE copolymer films. Two years later, Giegerich et al. [18] also showed improved piezoelectric behavior in similar polymers upon irradiation. However, these works suggested that a polarization step after irradiation is needed due to heating (i.e. induced depolarization) during radiative treatment. Nowadays, novel e-beam accelerators propose to drastically limit the heating during irradiation runs. In previous work [15], we have reported that it was effectively possible to treat polarized β-PVDF films by e-beam without affecting the remanent polarization. To do this, irradiation experimental conditions were adjusted to minimize the temperature increase. In the present work, we will strengthen this important experimental adaptation.

At first glance, radiative treatment may look rather complex. However, one should know that international facilities such GANIL offers industrial beam-lines allowing to rapidly treat hundreds of square meters of commercially poled PVDF film rolls of 50 cm wide. It is even easier to treat polymer films from e-beam irradiations facilities. The present paper reports on the piezoelectric response of β-PVDF/Ni NWs nanocomposites thin films, previously fabricated using our method by SHI nanostructuration, upon e-beam irradiation. We will investigate the effect of e-beam irradiation in very large dose range, up to 2.5MGy.

2. Material and methods

2.1. Sample preparation

Polarized thin bi-oriented β-PVDF films were purchased from PIE-ZOTECH SA (around 10 μm thick). These films were first irradiated under He atmosphere by swift heavy ion bombardment at GANIL, France. The ion-beam was composed of Kr^{36+} ions at energy of 10.37 MeV/u. A fluence of 5.10^8 cm^{-2} was chosen for all the samples. During its passage through the entire thickness of β-PVDF films (irradiation angle was normal to film surface), each Kr^{36+} ion created, all along its trajectory, a cylindrical and straight zone of damages, called latent track. Once the radiative treatment has been done, rolls are stored sealed in plastic bags under vacuum or any inert gas such as nitrogen in a freezer at −18 °C without special care. Using this storage procedure, no aging effects were observed years after irradiation campaigns. The ion latent tracks were then revealed by chemical etching for 30 min at 65 °C in KOH 10 N / KMnO$_4$ 0.25 N alkaline solution resulting in cylindrical nanopores of 50 nm of diameter and 10 micrometer long. The nanopore density was equal to the ion fluence. All nanopores were parallel to each other (deviation angle < 1%). These nanopores of high aspect ratio were subsequently filled of Ni(0) by electrodeposition using an acidic NiSO$_4$ (0.84 M) solution following exactly the same procedure described in detail in [14]. The length of the resulted Ni NWs embedded in the PVDF nanoporosity was proportional to electrodeposition time. Ni growth rate was 2.25 μm per 50 s of electrodeposition time. Three different sets of samples were obtained for 50, 100 and 150 s of electrodeposition corresponding to Ni NWs length of 2.25, 4.50 and 6.25 μm respectively. After electrodeposition, a 10 nm Al$_2$O$_3$ atomic layer was deposited on the top of the grown Ni nanowires (NWs) to avoid any short-circuit with the Au layer sputtered on top at the very end of the process. The resulting samples displayed a series of vertically aligned Ni NWs embedded in piezoPVDF films. The ensemble is sandwiched between two gold layers, one of 200 nm connected to the NWs (bottom) and one of 100 nm covering the Al$_2$O$_3$ atomic layer (top).

2.2. E-beam irradiation

E-beam irradiations were performed at SIRIUS facility (LSI, France) which is a 2.5 MeV pelletron accelerator purchased from NEC. Two dose rates of 50 and 500kGy.h^{-1} were used. The sample holder, named IRRAPLAST, allows irradiation of PVDF foils of 2 × 12 cmxcm under constant Helium atmosphere. The e-beam size is 2.5 × 1 cmxcm and the sample holder is moving in the horizontal direction. PVDF foils were scanned several times until the desired dose was reached. Scan-rate was adjusted to the sample size to stop once the foils have completed a run. A stack of no more than two foils was done. Subsequent characterizations and piezoelectric experiments were performed at least one month after the e-beam treatment.

2.3. Characterization by Electron microscopes (FESEM and TEM)

Electron microscopy with field emission scanning (FESEM) (Model HITACHI S-4800) at 2 kV accelerating voltage, 10 μA probe current, 30 mm working distance, mixing both upper and low detectors, was employed to measure the pore diameter and the mean length of NW Ni. No supplementary metal sputtering was necessary to image the samples. Transmission Electron Microscopy (TEM) imaging was performed using a JEOL2010 F TEM, equipped with a field emission gun operating at 80 keV. Samples were first freeze-dried and cut in thin slices using a Leica EM UC7 ultra-cryomicrotome.

2.4. Piezoelectric experimental set-up

As previously reported [14] using a home-made set-up, the piezo-potential of nanostructured composite Ni/piezoPVDF films is registered after mechanical strain applied by gas-pressure in a two-compartment cell. The set-up is composed of: a ISO-TECH DC (IPS 303DD) power supplier, a KEITHLEY 3390 waveform generator, a PicoScope 4000 series (input impedance 1MΩ) and a GEMS pressure sensor (output 0−5 V, range 0−2.5 bar). The argon arrival pressure was monitored with a 3-ways SMC VDW250 solenoid valve. The overall set-up is driven by Python scripts.

Each measurement has been repeated 50 times (or 50 cycles). One cycle means one bending and one release of piezoelectric film under Ar gas pressure with opening and closing of gas arrival driven by solenoid valve. The frequency of mechanical solicitations and the load resistance can be easily varied. Notably load resistance was adjusted for a series of samples in order to stay in the limit of 5 V imposed by the electronics. An example of piezopotential response of piezoelectric PVDF foil for 10
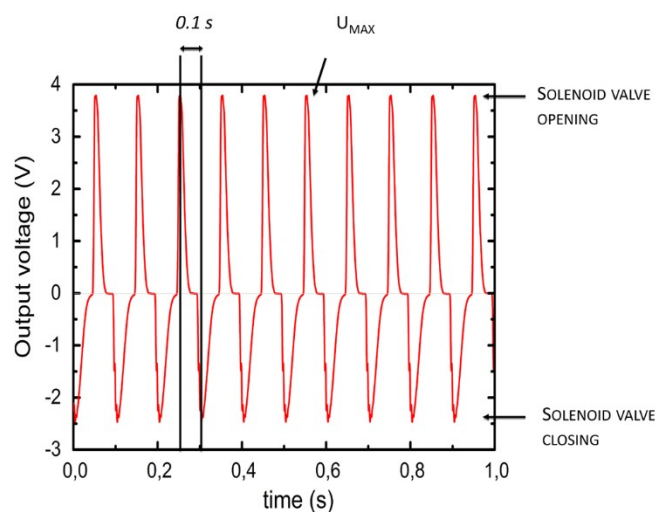

Fig. 1. Example of piezopotential response during poled PVDF deformation under following conditions: f = 10 Hz, R = 1MΩ, C = 220 nF, P = 0.58 bar.

cycles generating an alternative current (AC) is presented (Fig. 1). As our set-up registers simultaneously the generated current I corresponding to each output voltage U [see supplementary information], we can thus estimate the maximum of generated power P_{max} at output voltage peak maximum U_{max} taking into account the resistance of the circuit : $P_{max} = U_{max} \cdot I_{max}$.

2.5. Electron paramagnetic resonance

EPR measurements were done with JES-X310 equipment from JEOL. Power: 2 mW, field width: 40 m T, acquisition time: 30 s; modulation width: 0.5 m T; amplitude: 6; time constant: 0.1 s.

2.6. Differential scanning calorimeter

In order to obtain the heat of fusion and melting temperature to finally correlate it with the dose of irradiation Differential Scanning Calorimeter (DSC-7) measurement using Perkin-Elmer equipment with heating rate of 15 °C /min was done. The degree of crystallinity was calculated using the relationship:

$$X_c(\%) = \frac{H_f}{H_{f0}} \cdot 100$$

where H_f is the heat of fusion of the tested sample, and $H_{f0} = 104.$ J/g the heat of fusion of the 100 % crystalline sample [19].

2.7. Fourier-transform infrared spectroscopy (FT-IR)

The FT-IR examination was performed on polymer films using Nicolet IS50 spectrometer equipped with a DTGS detector. The sample compartment is kept under nitrogen flow. Placing the sample at Brewster's angle allows to obtain high quality transmission spectra in eliminating the interference fringes. The background acquisition was performed before each measurement. Spectra were collected by accumulation 32 scans at a resolution of 2 cm^{-1}. The wavenumber from 2000−500 cm^{-1}, was the range of choice that consists in polymer skeletal bending region.

The fraction of β-phase present in each sample could be calculated as follows [18]:

$$F(\beta) = \frac{A_\beta}{1.26 A_\alpha + A_\beta}$$

Where A_α and A_β corresponds to the areas of absorption bands of α and β, in our case 766 cm^{-1} and 840 cm^{-1}.

2.8. Elasticity measurements

The elastic modulus was evaluated by tensile test. The measurement was done using tensile test machine Instron 3342 with software Instron. The PVDF film (with length around 9 cm) was fixed between two grips and stretched in a uniaxial direction. The measurement was performed at constant strain rate (2 mm/min) at ambient temperature. The foil was stretched until break. During this process, the elongation of the film was recorded versus applied force. The strain in the material S is calculated from the measured elongation as,

$$S = \frac{L - L_0}{L_0}$$

where L_0 and L corresponds to initial and final length, respectively.

3. Results and discussion

The constitutive equations of piezoelectricity as written by Curie brothers in 1880 can be expressed as follows:

$$D = \varepsilon^T E + d_{33} T$$

$$S = d_{33} E + s^E T$$

where D represents the electric displacement (C. m^{-2}), E, the electric field (V. m^{-1}), T, the stress (N. m^{-2}), S, the strain, ε^T, the dielectric constant, s^E, the compliance (inverse of Young's modulus Pa^{-1}), d_{33}, the piezoelectric constant (m.V^{-1} or C.N^{-1}) in z direction.

PVDF/Ni NWs nanocomposite films were fabricated following the experimental protocol described in [14] (see also experimental section) to enhance the dielectric constant ε^T. Piezoelectric PVDF/Ni NWs composite thin films were synthesized from electrodeposition of Ni(II) ions inside the nanopores of a poled PVDF ion-track-etched membrane (Scheme 1).

An improvement of the piezoelectric response has already been reported using this approach. [14] The purpose is now to play on the compliance of the material by inducing damage in the polymer. To this aim, the PVDF nanocomposite was subjected to e-beam irradiation through its entire thickness. Radiation-induced damages lead to irreversible and over-time stable defects in the solid material.

The piezoelectric response of irradiated composites was directly studied in sensor mode. To do this, an Ar-pressure on the top of golden PVDF/Ni NWs composite thin films was cyclically applied to deform the films. Generated voltages were simultaneously registered. Fig. 2a shows the experimental set-up we used and Fig. 2c displays a typical registered output voltage profile. As shown by the pressure variation, the system electrically works only when composite films are subjected to deformation.

In Fig. 3, the output voltage corresponds to the average value of peak maxima of 50 cycles when opening solenoid valve (positive voltage signals). These average values were plot versus pressure at various doses. A dose range of 0–2.5MGy was investigated. Before any e-beam treatment, in agreement with previous results [14], the output voltage was enhanced by a factor 2.1 when filling the initial track-etched poled PVDF membrane with Ni NWs (Fig. 3a). The presence of Ni metallic inclusions in the poled PVDF improves the output voltage profile versus pressure without affecting the initial polarization of nanoporous track-etched PVDF.

The remanence of PVDF polarization after irradiation was herein evidenced up to 1000kGy. Even at 2500kGy (or 2.5MGy), a piezoelectric response was still registered but less effective as the composite became brittle and broke at 1 bar. Such a behavior suggests that, radiation-induced defects in the material provoked many damages which severely impacts on the material integrity. Despite, e-beam irradiation did not affect the dipolar momentum of the initial poled semi-crystalline PVDF film as voltage output was still measurable.

Irradiating with e-beam, a beneficial synergy resulting of an additional 1.4 times enhancement of output voltage was clearly evidenced between radiation-induced defects in the PVDF and Ni nanostructuration (Fig. 3a). The output voltage was maximum (U_{max}) for PVDF/Ni NWs composite foils submitted to 1 bar of pressure and irradiated at 1MGy. U_{max} was found equal to 4.1 V.cm^{-2} which corresponded to a maximum output power of roughly 25 μW. cm^{-2} (registered current I_{max} was 6 μA -see supplementary information-). The integrated power output over time was equal to 0.36μW for 0.78cm^{-2} resulting in a power density of 0.46μW. cm^{-2}. The pressure was intentionally limited above 1 bar to ensure staying in the elastic region of PVDF allowing a constant cycling. Fig. 3b shows that Ni NWs of middle length of around 4.5 μm (PVDF film thickness of around 10 μm) gave the best results. This phenomenon was maintained even at 1MGy.

The exceptional remanence of polarization without any additional poling step after irradiation is partially due to our irradiation experimental conditions. It is indeed important to note that the irradiation set-up, named IRRAPLAST at the 2.5 MeV e-beam SIRIUS international facility, allows to irradiate under a constant e-beam scanning and a
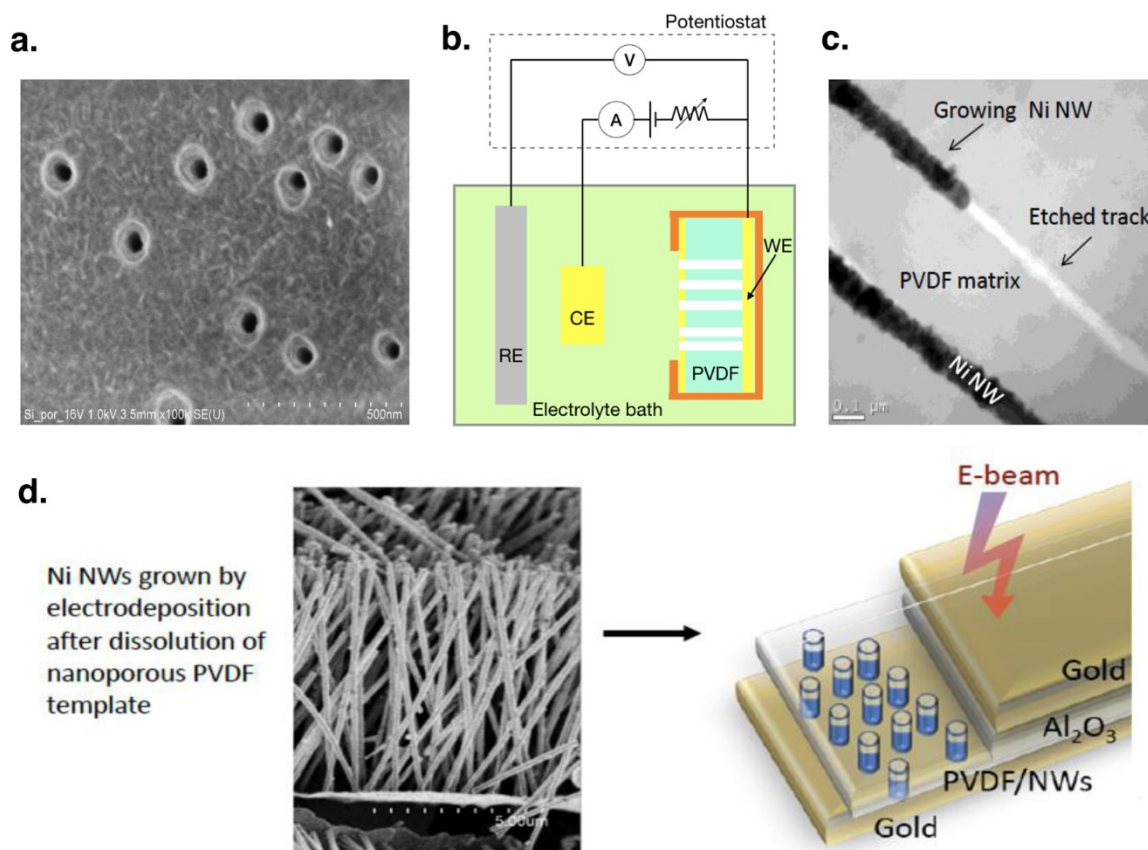
Scheme 1. a. FESEM image of a nanoporous β-PVDF ion-track-etched membrane obtained from SHI irradiation of Kr^{36+} (10 MeV/mau, fluence of 5.10^8 cm^{-2}) and subsequent chemical etching in alkaline $KOH/KMnO_4$ solution; b. Electrodeposition set-up principle : reduction of Ni salts inside PVDF nanopores was performed applying −1 V on the gold working electrode (WE) - c. TEM image of embedded Ni NWs in PVDF after electrodeposition (ultracryomicrotome cutting); d. Sketch of the final PVDF/Ni NWs composite film displaying multiple layer arrangement and FESEM image of Ni NWs in place - density of 5.10^8 cm^{-2} - (the PVDF membrane was dissolved in hot DMF prior imaging)- The ensemble is treated by e-beam irradiation.

continuous He atmosphere replacement. These special conditions permit to drastically limit the temperature increase inside the irradiation chamber. To know exactly which temperature was undergone by samples during irradiation, a thermocouple was stuck on a PVDF film immobilized inside the IRRAPLAST sample holder made of aluminium frame (Fig. 4a). A registered mild temperature range of 20–40 °C was measured at two different dose rates, namely 250kGy.h⁻¹ and 500kGy. h^{-1} as used to reach all the doses for the present study (Fig. 4b). A depolarization due to heating was thus avoided.

However, as abovementioned for 2.5MGy, the mechanical properties of composite films were highly affected with the dose. Upon irradiation, many chain scissions occurred in the polymeric part of the composite materials. Chain scissions resulted in radical formation [20]. The created radicals, alkyls and peroxyls ones, were trapped inside the crystalline part of PVDF polymer and can be easily observed by EPR after irradiation at room temperature (Fig. 5). The radical content was proportional to the dose. The obtained results suggest that chain scissions continuously increase with the dose. It is important to mention that EPR gives a footprint of what happens when radicals were initially created. A more important amount of radicals were firstly created and part of them rapidly disappeared by migration and recombination leading to crosslinks in the material. Thus, the irradiated polymer film is a mixture of broken chains and their unpaired electrons (radicals) and crosslinks.

By DSC (Fig. 6a), the irradiation damages on the crystallite size due to chain scissions were clearly evidenced with a dramatic decrease and broadening of melting temperature from 170 °C to 155 °C.

This observation is in agreement with previous studies [21–23]. The drop in the melting peak was attributed to reorganization of thicker lamellae. It has also been observed that a further increase in the dose of irradiation intensifies crosslinking and oxidative degradation in membranes (elimination of HF and peroxidation). This led to the formation of a crystalline structure in which the reorganized thicker lamellae completely disappeared [22].

Integrating melting peak area, the degree of crystallinity was also plotted (Fig. 6b). What is interesting is that the relationship is not linear and depends on the dose. In agreement with previous work [15], a slight increase of crystallinity content can be observed up to 10 kGy. The gel dose of PVDF is known to occur in the range of 10−20kGy [24,25]. Before the gel dose, chain scissions are predominant. Smaller chains can better reorganize to form new crystallites. Then, increasing the dose, crosslinking became predominant in the gel dose range reducing polymer chain mobility and limiting new crystallite formation. At very high dose range from 200kGy to 1MGy, even if the crystallinity content was not so dramatically affected (still 38 % of crystallinity at 1MGy), a slight decrease of the degree of crystallinity was initiated. Indeed, for doses superior to 10MGy, the damages are expected to result in an important amorphization as shown by Betz et al. [26] in PVDF polymer matrix.

As β-phase is responsible for PVDF piezoelectric properties, a FT-IR analysis permits to evaluate the β phase fraction in our PVDF foils. PVDF is known to be polymorph and many crystalline phases (α, β, γ, δ) are simultaneously present. Herein, purchased bi-stretched poled PVDF films content more than 80 % of β-phase. The rest was principally composed of α phase, the thermodynamically stable phase which was initially predominant before stretching.

At first, it is important to know whether a large dose of irradiation such as 1000 or 2500kGy leads to the destruction of some polymer
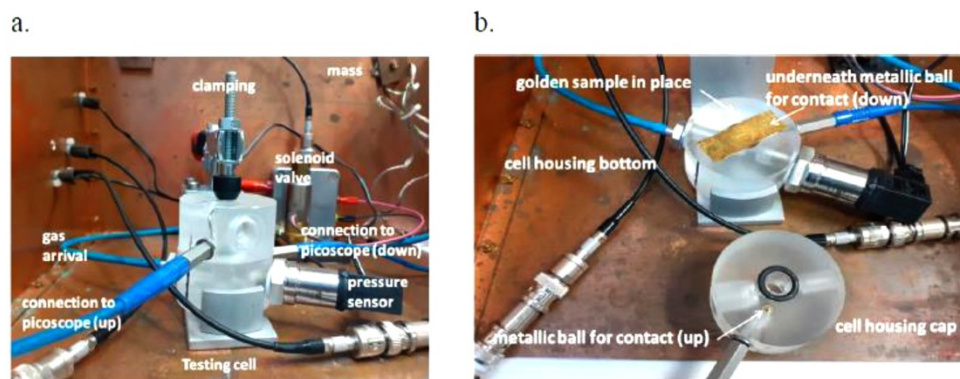
a.

b.

Fig. 2. a. experimental set-up allowing the simultaneous registration of the Ar gas pressure and the output voltage; b. open cell of 0.78 cm^2 with a gold sample in place; c. typical registered piezoelectric signal of Ni NWs/PVDF thin composites using our experimental set-up (f = 10 Hz, R$_{load}$ = 500kΩ). The output voltage is registered between gold surfaces via metallic balls included inside the PMMA cell housing; the pressure profile applied during one cycle results from the opening and closing of the solenoid valve driving Ar gas arrival. The gas pressure is measured using a pressure sensor placed inside the cell. The mechanical solicitation frequency was set here to 10 Hz (peak-to-peak time of 0.1 s).
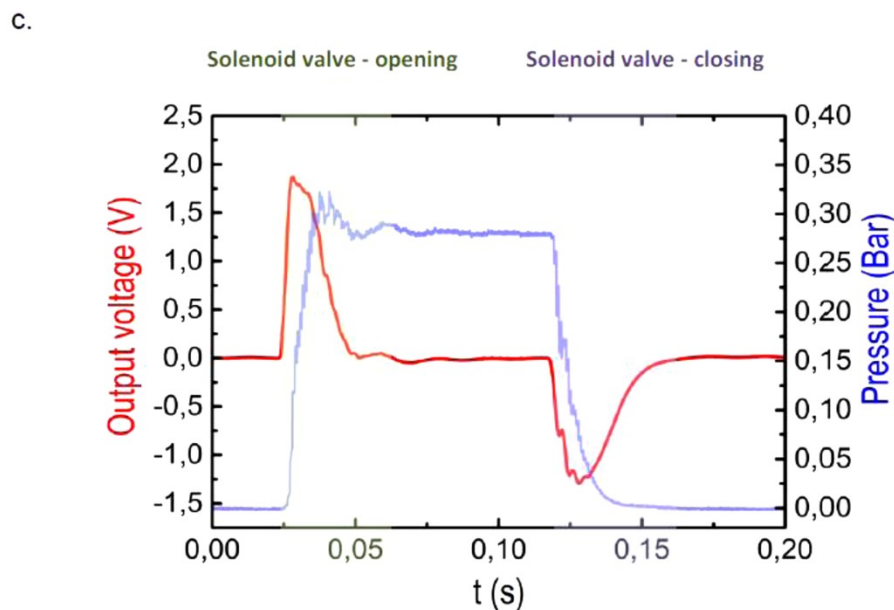
c.

a.

b.
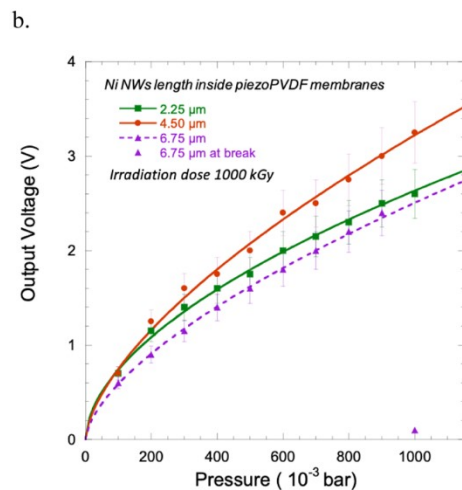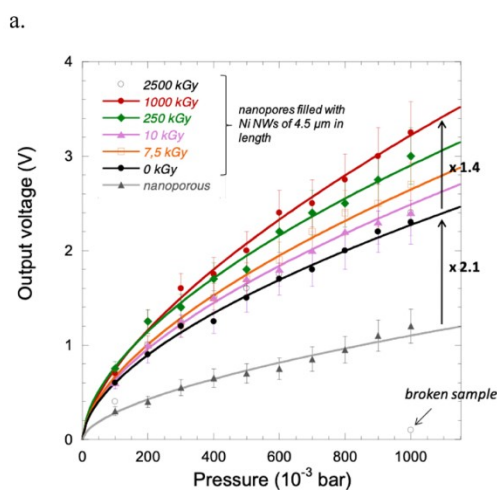
Fig. 3. Piezoelectric response as function of a. various dose of irradiation and b. different Ni NWs length at dose 1000 kGy (mechanically solicitated composite surface = 0.78cm^{-2}) - continuous lines correspond to empirical power law curve fits - f = 10 Hz, R$_{load}$ = 500kΩ..

crystal phases. According to obtained FT-IR spectra, it can be stated that no dramatic structural differences were detected (Fig. 7a). Considering the polymer skeleton vibration region between 900 and 400 cm^{-1}, peak assignment is consistent with previous work, 840 and 510 cm^{-1} for β and 766, 615 and 532 cm^{-1} for α. [15] α and β phases were predominant

in our PVDF films. Some γ-phase peaks may also be assigned. However, these peaks are subject to discussion as they cannot be only assigned to this crystal phase but also to other bond vibration modes coming from polymer amorphous phase. It ought to be stressed that the δ-phase was not visible. This phase is a polarized version of α phase and usually needs
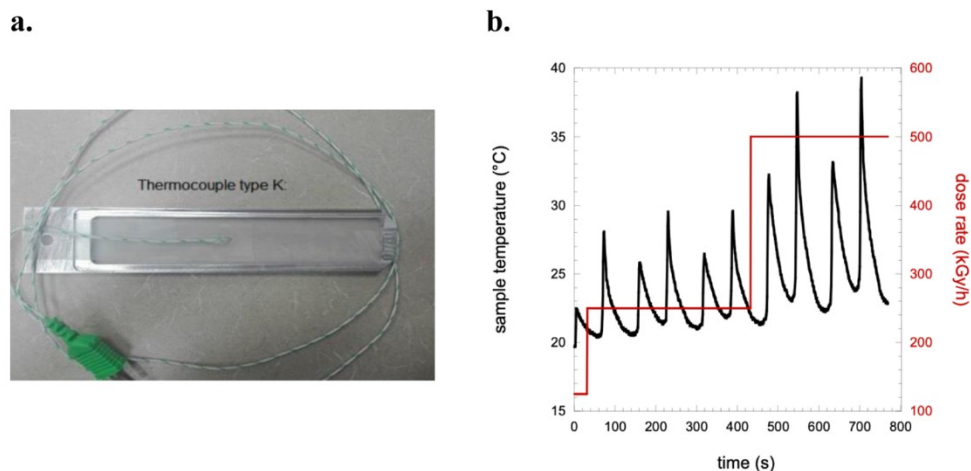
a.

b.

Fig. 4. a. IRRAPLAST samples holder with a PVDF film in place and a flexible thermocouple sticked along PVDF film; b. Registered sample temperature at two dose rates: 250 and 500 kGy. h^{-1} - one run corresponds to one e-beam scan -.
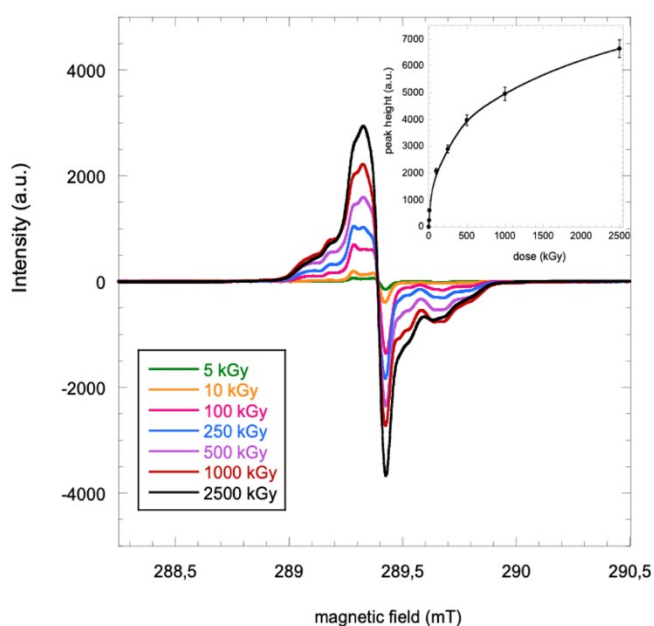

Fig. 5. EPR spectra of e-beam irradiated piezoPVDF films at various doses; inset: peak height versus dose.

high electric field to be formed [27]. The initial poling was then not strong enough to generate such crystal phase.

The content of β fraction was calculated according to equation shown in experimental part (see section 2.7). It should be emphasized that the peak assignment for calculation of β to α ratio is still under discussion [28]. The debate comes from the close proximity of the peaks and the coexisting connections between the crystalline phases. Despite the fact that for many years the 532 cm^{-1} peak corresponding to α-phase was used in the calculations, as suggested by Salimi et al. [29], recent scientific studies [28,30] advice to use the peak at the 766 cm^{-1} instead, due to its better separation in comparison with other overlapping peaks. The calculation of β fraction was then done using absorption FT-IR bands at 766 and 840 cm^{-1} corresponding to pure α and β phases respectively. Based on this calculation, β-phase fraction was lowered when PVDF films were irradiated compared to reference sample (Fig. 7b). Initial β-phase fraction of 82 % stated the significant participation of piezoelectric active phase in studied material. Then, the β to α fraction decreases until 60 % when reaching a dose of 100kGy followed by a slower increase to 80 % up to 2500 kGy. At low doses, the sharp decrease may be due to α-phase formation provoked by chain scissions reorganization corresponding to observed increase of crystallinity degree by DSC. At higher dose, the slow increase suggests that β to α phase ratio results in more α-phase damages by irradiation and perhaps some chains reorganization in β-phase. However, this β to α fraction evolution with the dose cannot explain the important piezoelectric response observed at 1MGy in our composite material. It seems that the parameter responsible for
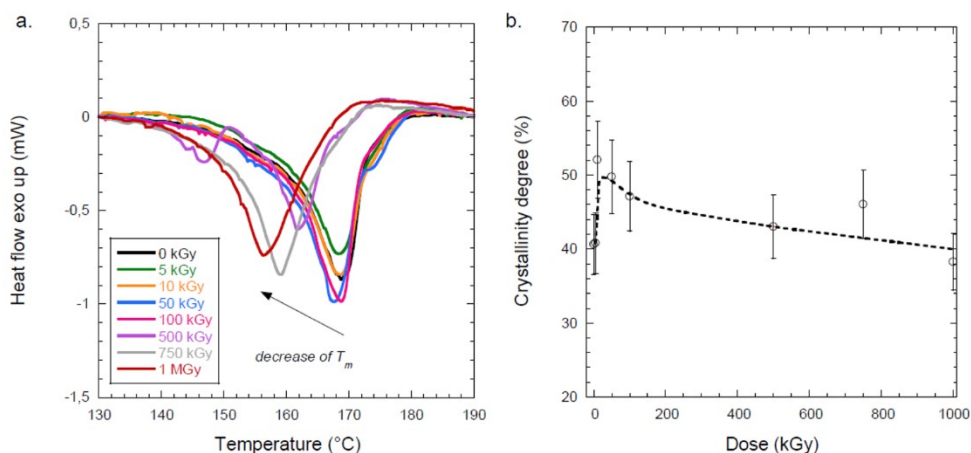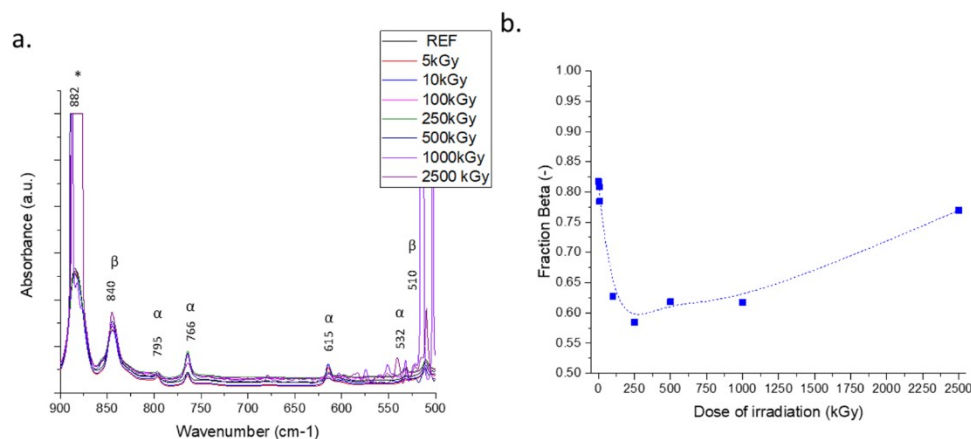

Fig. 6. a. DSC melting peak for PVDF polymer films treated by different dose of irradiation, b. percentage of crystallinity in function of irradiation dose.

Fig. 7. a. Comparison with FT-IR spectra of irradiated PVDF polymer in dose range of 5-2500 kGy and reference sample, b. β fraction as function of irradiation dose.

such an effect is not only the β fraction content but it should also be associated with an increased polymer deformation upon strain due to enhanced polymer chain mobilities.

To understand how the elastic component of PVDF is affected by irradiation, further studies were carried out employing tensile tests. Table 1 displays Young's moduli obtained in the elastic region of PVDF films.

Young's modulus variations exhibited more or less the same variations as the degree of crystallinity. It effectively reflects a non-negligible rigidity due to crystal content increase above 10kGy. It confirms that, at low doses, shortened polymer chains created by e-beam damages were reorganized into new crystallites. In the range from 10kGy to 1MGy the polymer recovers its initial elasticity. The elasticity was more or less constant. At 2500kGy, higher values of Young's modulus were measured (Table 1). The material became brittle. The rigidity was clearly seen with broken samples during piezoelectric tests for irradiated sample at 2500kGy. It indicates that severe e-beam damages caused many depolymerization destroying the material integrity.

To limit the material damages as just its need for elasticity improvement and good piezoelectrical response, a good compromise was to limit irradiation impact investigation until 500kGy, which corresponds to the maximum of compliance, s^E. A laser was also placed through a pinhole drilled in the upper cell housing of our experimental set-up to measure piezoPVDF films displacement while applying pressure and simultaneously registering generated output voltage. In Fig. 8, it was evidenced that increasing the dose of irradiation, the displacement gradually increased. The deformation upon pressure of irradiated PVDF was consequently enhanced.

It is worth noticing that the increased deformation obtained by irradiation brought better piezoelectric efficiencies for the low displacement mode in comparison to untreated poled PVDF. This result is very interesting when dealing with renewable energies as the expected pressures coming from environmental vibrations are not always in the optimum pressure range.

Table 1
Young's moduli Y and corresponding compliances s^E of irradiated PVDF films obtained by tensile test.

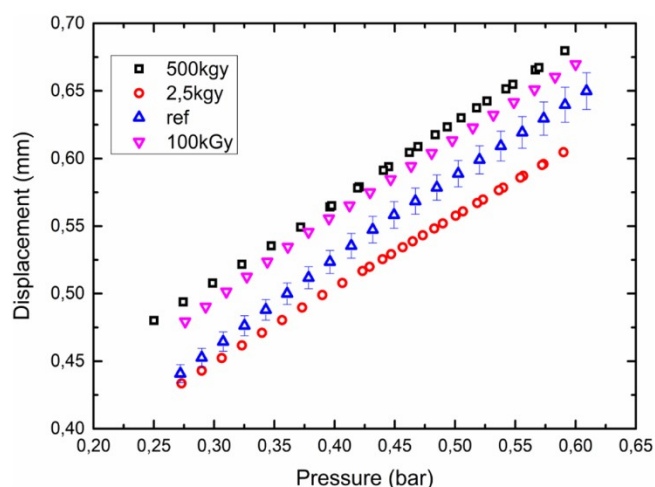| Dose (kGy)	Y (MPa)	s^E (10^{-3} MPa^{-1})
0	508 ± 40	1.97
5	700 ± 22	1.43
10	504 ± 12	1.98
100	539 ± 55	1.85
250	556 ± 25	1.80
500	445 ± 101	2.25
1000	508 ± 35	1.97
2500	596 ± 18	1.68

Fig. 8. Measured displacement of PVDF films plotted against the applied pressure in the experimental cell used for piezoelectric response registration.

Exhibiting almost parallel linear behaviors whatever the e-beam irradiation dose, the Fig. 8 gave us a conversion, pressure to displacement, ΔL/ΔP. Up to 1 bar pressure, the polymer deformation was in the elastic and reversible part of tensile strength curves. It is worth noting that the slopes ΔL/ΔP exhibits slight variations which can be nicely correlated to Young's modulus variations with the dose (Fig. 9).

Despite radiation-induced damages result in crystallite breaks as observed by DSC (Fig. 6a), the amount of amorphous phase is globally unchanged (Fig. 6b). It reversely induces a slight increase of 10 % of crystallinity, especially before the dose-gel of PVDF at 10kGy. Young's modulus reflects this increase of crystallinity below10kGy in exhibiting a peak well-above error bars (inset of Fig. 9).

The decrease of Young's modulus at 500kGy evidences the highest deformation (Fig. 9). This may suggest that one of the key parameters for a higher energy harvesting for piezoelectric composite polymer foils is a higher deformation under strain. However, above 500kGy up to 2.5MGy, the material looses the benefit of softening effect provided by e-beam damaging and become brittle. At the light of this observation, it seems that the polymer chain re-organization in favor of β-phase content under e-beam irradiation up to 1MGy as shown by FTIR cannot be minimized. In such large dose range, both phenomena explain the additional enhanced piezopotential response of composite PVDF/Ni NWs foils once submitted to e-beam irradiation as shown in Fig. 3.
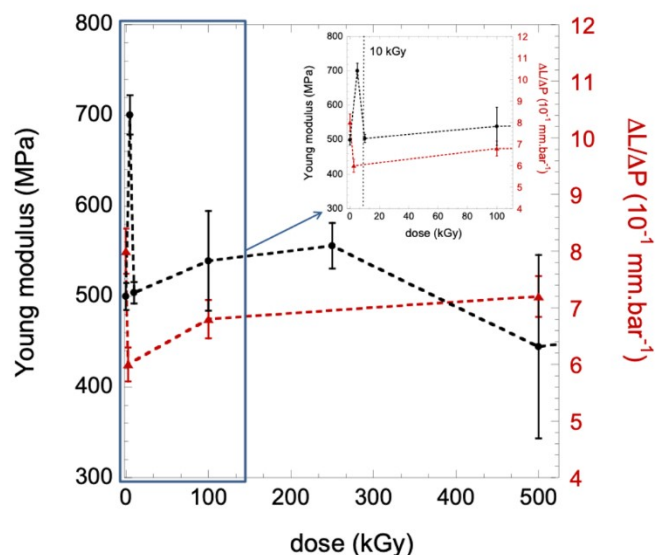
Fig. 9. Comparison between Young's modulus variations and deformation induced by pressure with the dose; inset: mirror effect in the low dose range with strong variation of Young's modulus and corresponding polymer displacement with pressure.

4. Conclusion

The results presented in the discussed work indicate that successive irradiative treatments, nanostructuration by SHI and e-beam irradiation, significantly modify the properties of piezoelectric PVDF/Ni nanostructured composites foils. The beneficial effect of both e-beam irradiation damages and embedded metallic nanowires, enhancing the dielectric permittivity, was confirmed. Synergies of both treatments lead to a total output voltage improvement of 3.5 times in comparison to untreated poled nanoporous PVDF films. The important piezoelectric response up to 1MGy resulted in a balance between a higher PVDF compliance provoked by smaller crystallite size and shortened polymer chains re-organization into β-phase crystallites. Nevertheless, at 1MGy, the damages in the polymer films were tremendous, even if not as dramatic as it was at 2.5MGy. The durability of the material may thus be thrown into serious question. To limit the material damages as just its need for elasticity improvement and good piezoelectrical response, a good compromise for material use in industrial devices would be to limit irradiation treatment to doses until 500kGy.

In this study, the pressure was intentionally limited above 1 bar to ensure staying in the elastic region of PVDF polymer during deformation cyclings. Such a polymer matrix is able to undergo more strain without exhibiting irreversible creep. It means that there is still room for further optimizations in exploring higher pressure range and harvest even more energy.

Author statement

Natalia Potrzebowska: samples characterization and writing contribution; **Olivier Cavani :** e-beam irradiations ; **Ozlem Oral :** technical assistance ; **Olivier Doaré :** Young modulus measurements ; **Giuseppe Melilli :** samples fabrication; **Jean-Eric Wegrowe :** nanowire grown by template synthesis expert and writing contribution; **Marie-Claude Clochard:** piezoelectric measurements, writing contribution and project coordinator.

Declaration of Competing Interest

The authors declare that they have no known competng financial interests or personal relationships that could have appeared to influence the work reported in this paper.

Appendix A. Supplementary data

Supplementary material related to this article can be found, in the online version, at doi:https://doi.org/10.1016/j.mtcomm.2021.10 2528.

References

[1] Y. Liu, G. Tian, Y. Wang, J. Lin, Q. Zhang, H.F. Hofmann, Active piezoelectric energy harvesting: general principle and experimental demonstration, J. Intell. Mater. Syst. Struct. 20 (5) (2008) 575–585, https://doi.org/10.1177/1045389X08098195.

[2] D. Vatansever, R.L. Hadimani, T. Shah, E. Siores, An investigation of energy harvesting from renewable sources with PVDF and PZT, Smart Mater. Struct. 20 (5) (2011), 055019, https://doi.org/10.1088/0964-1726/20/5/055019.

[3] Z. Cui, N.T. Hassankiadeh, Y. Zhuang, E. Drioli, Y.M. Lee, Crystalline polymorphism in poly(Vinylidenefluoride) membranes, Prog. Polym. Sci. 51 (2015) 94–126, https://doi.org/10.1016/j.progpolymsci.2015.07.007.

[4] M. El Achaby, F.Z. Arrakhiz, S. Vaudreuil, E.M. Essassi, A. Qaiss, Piezoelectric β-Polymorph formation and properties enhancement in graphene oxide – PVDF nanocomposite films, Appl. Surf. Sci. 258 (19) (2012) 7668–7677, https://doi.org/10.1016/j.apsusc.2012.04.118.

[5] B. Mohammadi, A.A. Yousefi, S.M. Bellah, Effect of tensile strain rate and elongation on crystalline structure and piezoelectric properties of PVDF thin films, Polym. Test. 26 (1) (2007) 42–50, https://doi.org/10.1016/j.polymertesting.2006.08.003.

[6] R.A. Surmenev, R.V. Chernozem, I.O. Pariy, M.A. Surmeneva, A review on piezo- and pyroelectric responses of flexible nano- and micropatterned polymer surfaces for biomedical sensing and energy harvesting applications, Nano Energy 79 (2021), 105442, https://doi.org/10.1016/j.nanoen.2020.105442.

[7] L.J. Lu, W.Q. Ding, J.Q. Liu, B. Yang, Flexible PVDF based piezoelectric nanogenerators, Nano Energy 78 (2020), 105251, https://doi.org/10.1016/j.nanoen.2020.105251.

[8] R. Hayakawa, Y. Wada, Piezoelectricity and related properties of polymer films, in: Fortschritte Der Hochpolymeren-Forschung. Advances in Polymer Science, Vol. 11, Springer, Berlin, Heidelberg, 1973, pp. 1–55, https://doi.org/10.1007/3-540-06054-5_10.

[9] A. Nafari, H.A. Sodano, Tailored nanocomposite energy harvesters with high piezoelectric voltage coefficient through controlled nanowire dispersion, Nano Energy 60 (2019) 620–629, https://doi.org/10.1016/j.nanoen.2019.03.097.

[10] S.-R. Kim, J.-H. Yoo, J.H. Kim, Y.S. Cho, J.-W. Park, Mechanical and piezoelectric properties of surface modified (Na,K)NbO3-based nanoparticle-embedded piezoelectric polymer composite nanofibers for flexible piezoelectric nanogenerators, Nano Energy 79 (2021), 105445, https://doi.org/10.1016/j.nanoen.2020.105445.

[11] S. Cha, S.M. Kim, H. Kim, J. Ku, J.I. Sohn, Y.J. Park, B.G. Song, M.H. Jung, E.K. Lee, B.L. Choi, J.J. Park, Z.L. Wang, J.M. Kim, K. Kim, Porous PVDF as effective sonic wave driven nanogenerators, Nano Lett. 11 (12) (2011) 5142–5147, https://doi.org/10.1021/nl202208n.

[12] B. Stadlober, M. Zirkl, M. Irimia-Vladu, Route towards sustainable smart sensors: ferroelectric polyvinylidene fluoride-based materials and their integration in flexible electronics, Chem. Soc. Rev. 48 (6) (2019) 1787–1825, https://doi.org/10.1039/C8CS00928G.

[13] C. Lee, H. Park, J.-H. Lee, Recent structure development of poly(Vinylidene fluoride)-based piezoelectric nanogenerator for self-powered sensor, Actuators 9 (3) (2020) 57, https://doi.org/10.3390/act9030057.

[14] G. Melilli, D. Gorse, A. Galifanova, O. Oral, E. Balanzat, O. Doare, M. Tabellout, M. Bechelany, D. Lairez, J.-E. Wegrowe, M.-C. Clochard, Enhanced piezoelectric response in nanostructured Ni/PVDF films, J. Mater. Sci. Eng. 7 (2018) 2, https://doi.org/10.4172/2169-0022.1000444.

[15] G. Melilli, D. Lairez, D. Gorse, E. Garcia-Caurel, A. Peinado, O. Cavani, B. Boizot, M.-C. Clochard, Conservation of the piezoelectric response of PVDF films under irradiation, Radiat. Phys. Chem. 142 (2018) 54–59, https://doi.org/10.1016/j.radphyschem.2017.03.035.

[16] F. Cordero, Elastic properties and enhanced piezoelectric response at morphotropic phase boundaries, Materials 8 (12) (2015) 8195–8245, https://doi.org/10.3390/ma8125452.

[17] Q.M. Zhang, V. Bharti, X. Zhao, Giant electrostriction and relaxor ferroelectric behavior in electron-irradiated poly(vinylidene fluoride-trifluoroethylene) copolymer, Science 280 (5372) (1998) 2101–2104, https://doi.org/10.1126/science.280.5372.2101.

[18] U. Giegerich, J. Wust, B.-J. Jungnickel, The stability of ferroelectric polarization of PVDF upon irradiation, IEEE Trans. Dielectr. Electr. Insul. 7 (3) (2000) 353–359, https://doi.org/10.1109/94.848915.

[19] M.M. Nasef, K.Z.M. Dahlan, Electron irradiation effects on partially fluorinated polymer films: structure–property relationships, Nucl. Instrum. Methods Phys. Res. Sect. B Beam Interact. Mater. At. 201 (4) (2003) 604–614, https://doi.org/10.1016/S0168-583X(02)02068-2.

[20] M. Ferry, Y. Ngono-Ravache, C. Aymes-Chodur, M.-C. Clochard, X. Coqueret, L. Cortella, E. Pellizzi, S. Rouif, S. Esnouf, Ionizing radiation effects in polymers. Reference Module in Materials Science and Materials Engineering, Elsevier, 2016, https://doi.org/10.1016/B978-0-12-803581-8.02095-6. B9780128035818020000.

[21] M.M. Nasef, H. Saidi, K.Z.M. Dahlan, Investigation of Electron irradiation induced-changes in poly(Vinylidene fluoride) films, Polym. Degrad. Stab. 75 (1) (2002) 85–92, https://doi.org/10.1016/S0141-3910(01)00206-3.

[22] K.D. Pae, S.K. Bhateja, J.R. Gilbert, Increase in crystallinity in poly(Vinylidene fluoride) by Electron beam radiation, J. Polym. Sci. Part B: Polym. Phys. 25 (4) (1987) 717–722, https://doi.org/10.1002/polb.1987.090250402.

[23] Z. Tan, X. Wang, C. Fu, C. Chen, X. Ran, Effect of Electron beam irradiation on structural and thermal properties of gamma poly (Vinylidene fluoride) (γ-PVDF) films, Radiat. Phys. Chem. 144 (2018) 48–55, https://doi.org/10.1016/j.radphyschem.2017.10.018.

[24] N. Betz, Swift heavy ions effects in fluoropolymers: radicals and crosslinking, Nucl. Instrum. Methods Phys. Res. Sect. B Beam Interact. Mater. At. 116 (1–4) (1996) 207–211, https://doi.org/10.1016/0168-583X(96)00125-5.

[25] M.-C. Clochard, J. Bègue, A. Lafon, D. Caldemaison, C. Bittencourt, J.-J. Pireaux, N. Betz, Tailoring bulk and surface grafting of poly(Acrylic acid) in electron-irradiated PVDF, Polymer 45 (26) (2004) 8683–8694, https://doi.org/10.1016/j.polymer.2004.10.052.

[26] N. Betz, A. Le Moël, E. Balanzat, J.M. Ramillon, J. Lamotte, J.P. Gallas, G. Jaskierowicz, A FTIR study of PVDF irradiated by means of swift heavy ions, J. Polym. Sci. Part B: Polym. Phys. 32 (8) (1994) 1493–1502, https://doi.org/10.1002/polb.1994.090320821.

[27] M. Li, H.J. Wondergem, M.-J. Spijkman, K. Asadi, I. Katsouras, P.W.M. Blom, D. M. de Leeuw, Revisiting the δ-phase of poly(vinylidene fluoride) for solution-processed ferroelectric thin films, Nat. Mater. 12 (5) (2013) 433–438, https://doi.org/10.1038/nmat3577.

[28] X. Cai, T. Lei, D. Sun, L. Lin, A critical analysis of the α, β and γ phases in poly (vinylidene fluoride) using FTIR, RSC Adv. 7 (25) (2017) 15382–15389, https://doi.org/10.1039/C7RA01267E.

[29] A. Salimi, A.A. Yousefi, Analysis method: FTIR studies of β-Phase crystal formation in stretched PVDF films, Polym. Test. 22 (6) (2003) 699–704, https://doi.org/10.1016/S0142-9418(03)00003-5.

[30] Y. Ting, Suprapto, C.-W. Chiu, H. Gunawan, Characteristic analysis of biaxially stretched PVDF thin films, J. Appl. Polym. Sci. 135 (36) (2018) 46677, https://doi.org/10.1002/app.46677.